Facile Synthesis of Uniform Zinc-blende ZnS Nanospheres with Excellent Photocatalytic Activity toward Methylene Blue Degradation

PENG Si-Yan(彭思艳);YANG Liu-Sai(杨流赛);LV Ying-Ying(吕英英);YU Le-Shu(余乐书);HUANG Hai-Jin(黄海金);WU Li-Dan(吴丽丹)

School of Chemistry and Environmental Science, Jiangxi Province Key Laboratory of Polymer Preparation and Processing, Shangrao Normal University, Shangrao, Jiangxi 334001, *China*

ABSTRACT Uniform and well-dispersed ZnS nanospheres have been successfully synthesized via a facile chemical route. The crystal structure, morphology, surface area and photocatalytic properties of the sample were characterized by powder X-ray diffraction (XRD), scanning electron microscopy (SEM), Brunauer-Emmett-Teller (BET) and ultraviolet-visible (UV-vis) spectrum. The results of characterizations indicate that the products are identified as mesoporous zinc-blende ZnS nanospheres with an average diameter of 200 nm, which are comprised of nanoparticles with the crystallite size of about 3.2 nm calculated by XRD. Very importantly, photocatalytic degradation of methylene blue (MB) shows that the as-prepared ZnS nanospheres exhibit excellent photocatalytic activity with nearly 100% of MB decomposed after UV-light irradiation for 25 min. The excellent photocatalytic activity of ZnS nanospheres can be ascribed to the large specific surface area and hierarchical mesoporous structure.

Keywords: ZnS nanospheres, zinc-blende, photocatalytic activity, methylene blue, degradation;

DOI: 10.14102/j.cnki.0254-5861.2011-1721

1 INTRODUCTION

With the rapid development of textile dyeing industry, environmental wastewater pollution coming from various persistent and hazardous organic pollutants has attracted increasing attention in recent years. Over the past few decades, semiconductor photocatalysts are becoming more and more attractive due to their potential advantages such as cost-effective, easy operation, environment friendly, high efficiency, wide applicability and high chemical stability in resolving environmental wastewater pollution issues[1, 2]. The

semiconductor photocatalysis is also considered as one of the most effective methods in the degradation of pollutants because of the high reactivity of free radicals such as hydroxyl, which are originated from electron-hole pairs created in semiconductor materials by the absorption of photons[3].

ZnS is an important II-VI semiconducting material with a direct wide band gap. Due to its special electrical and optical properties, ZnS has been widely used in electroluminescence[4], field-effect transistors[5], solar cells[6], gas sensing[7], photocatalysis[8] and so on. Because of morphology-dependent property and increasing interest in morphology-controllable synthesis, ZnS materials with various morphologies, such as nanowires[9], nanobelts[10], nanorods[11], two-dimensional nanosheets[12] and three-dimensional flower-like architectures[13], have been fabricated in recent years. For photocatalysts, the hierarchical architectures would show superior photocatalytic efficiency, which can be ascribed to their high energy conversion efficiencies as well as light-harvesting capacities obtained by constructing the complex architectures[14]. Therefore, designing photocatalysts with hierarchical structures is of great importance to enhance the photocatalytic efficiency.

In this work, hierarchically uniform and well-dispersed zinc-blende ZnS nanospheres assembled by nanoparticles have been successfully achieved by a facile solution approach. The synthesized ZnS nanospheres can be employed as efficient photocatalysts (nearly 100% degradation ratio) for the degradation of methylene blue under UV-light irradiation. To the best of our knowledge, there have been few reports on the hierarchically uniform zinc-blende ZnS nanospheres composed of secondary nanoparticles with excellent photocatalytic performance.

2 EXPERIMENTAL

2. 1 Preparation of zinc-blende ZnS nanospheres and common ZnS

Preparation of zinc-blende ZnS nanospheres All chemicals were used as received without further purification. In a typical synthesis process, 3 mmol zinc acetate dehydrate was dissolved in 25 mL ethylene glycol under stirring to form a clear solution, and then 1 mL ethylenediamine was added into the solution before heating. When the solution was first heated to 100 °C, a freshly prepared 25 mL ethylene glycol solution containing 4.5 mmol thiourea was dropwise added into the solution. After the solution was further heated to 150 °C, 1 mL dodecylamine was quickly injected into the solution. The whole solution was kept at

150 °C for 3 hours. After cooling down to room temperature, the product was centrifuged, washed with ultrapure water and ethanol for several times, and then dried at 80 °C for 8 hours under vacuum.

Preparation of common zinc-blende ZnS In order to gain insights into the structure effect of ZnS nanospheres on the photocatalytic activity, common zinc-blende ZnS was prepared by the precipitation method for comparison. 3.6 g NaS $9H_2O$ (15 mmol) and 4.46 g $Zn(NO_3)_2$ $6H_2O$ (15 mmol) were completely dissolved in 15 mL deionized water, respectively, and then the two clear and colorless aqueous solutions were mixed together under stirring to form ZnS precipitate at room temperature. The product was centrifuged, washed with ultrapure water for several times, and then dried at 100 °C for 8 hours under vacuum.

2. 2 Characterizations

The morphologies of the sample were observed by scanning electron microscopy (SEM, JEOL JSM-6700F). The energy dispersive X-ray spectroscopy (EDS) analysis of the sample was measured using silicon wafer as the substrate on Field Emission Scanning Electron Microscope (Hitachi SU-8010). Powder X-ray diffraction (XRD) patterns were measured on a glass wafer by a Rigaku MiniFlex 600 diffractometer with a Cu-$K\alpha$ X ray source (λ = 1.5406 Å). UV-vis spectra were recorded on an Agilent Technologies Cary 60 spectrophotometer. The BET surface areas and pore size distributions of the samples were determined by N_2 adsorption-desorption at liquid nitrogen temperature (77 K), which was performed on a Micromeritics ASAP 2460 after the samples were degassed at 120 ℃ for 2 hours.

2. 3 Photocatalytic experiments

The photocatalytic activities of ZnS samples were carried out by the degradation of methylene blue (MB) aqueous solution with an initial concentration of 10 mg/L under the irradiation of two 8 W UV-light tubes (λ = 254 nm). 50 mg of catalyst powder was added to 50 mL of MB solution in a quartz cup, corresponding to a catalyst dosage of 1 g/L. Before UV-light irradiation, the whole system was placed in the dark under the magnetically stirring for 60 min to ensure an adsorption/desorption equilibrium. During the UV-light irradiation, about 4 mL aliquots were sampled at given time intervals, and centrifuged. Then the top clear solution of MB was analyzed by a UV-vis spectrophotometer (TU-1901, PERSEE, Beijing). The degradation ratio was monitored by measuring the absorption of MB at the wavelength of 664 nm, which was calculated according to the formula: $\eta = [(A_0 - A_t)/A_0] \times 100\%$, where A_0 is the absorbance of MB solution with the

initial concentration, and A_t is the absorbance of MB solution measured after photocatalytic degradation. For comparison, the blank control experiment (pure MB solution without catalyst under UV-light irradiation) was also determined in order to establish the effect of photolysis and catalysis on the conversion of MB.

3 RESULTS AND DISCUSSION

3. 1 Characterization

The morphology, structure and component of as-synthesized ZnS nanospheres and common ZnS were examined by electron microscopy techniques. Fig. 1a displays a low magnification SEM image of ZnS nanospheres, indicating that the obtained ZnS sample consists of uniform and well-dispersed nanospheres with an average diameter of 200 nm. The higher magnification SEM image (Fig. 1b) of ZnS nanospheres shows that the surfaces of nanospheres are rough. It suggests that nanospheres are likely assemblies of tiny nanoparticles. The EDS spectrum (Fig. 1c) indicates that the as-prepared ZnS nanospheres are only composed of Zn and S elements, while the signal for Si is from the substrate. The atomic ratio of Zn and S in ZnS nanospheres is approximately 47.42:52.58, close to the stoichiometric ratio of ZnS (1:1). As indicated by the SEM image in Fig. 1d, common ZnS obtained by the precipitation method is composed of nanoparticles aggregates. The sizes of these aggregates are not uniform, which are mainly above 200 nm.

The phase compositions of the as-prepared ZnS nanospheres and common ZnS were characterized by XRD. As seen in Fig. 2, all the diffraction peaks of both samples match well with the standard diffraction data for a cubic zinc blende structure of ZnS (JCPDS, No. 05-0566)[15]. No traces of extra diffraction peaks were detected, indicating the formation of a pure-phase structure in the as-prepared ZnS nanospheres and common ZnS. Three broad peaks are observed for both ZnS nanospheres and common ZnS at 2θ = 28.6, 48.2 and 56.7 °, which are assigned to (111), (220) and (311) characteristic diffractions, respectively[16]. The typical broadening of the three diffraction peaks indicates that ZnS nanospheres and common ZnS are comprised of many tiny constituent nanoparticles. The mean crystallite sizes of ZnS nanoparticles for ZnS nanospheres and common ZnS estimated by the Debye-Scherrer formula based on the peak (111) are ca. 3.2 and 2.1 nm, respectively, which are much smaller than those of both samples observed by SEM. It demonstrates that ZnS nanospheres and common ZnS are both assemblies of tiny constituent nanoparticles.

UV-vis spectrum is often applied to investigate the optical absorption properties of semiconductors. Fig. 3a presents the UV-vis absorption spectra of both ZnS nanospheres and common ZnS. Both ZnS samples show a

strong absorption edge in the ultraviolet region (310～360 nm), which can be assigned to the optical absorption edge of ZnS. It is seen that the absorption edge of ZnS nanospheres shifts toward a lower wavelength relative to common ZnS. The direct band gap energy (Eg) can be estimated from the UV-Vis spectra via a Tauc plot of $(\alpha h\nu)^2$ versus photon energy ($h\nu$) according to the Tauc relationship[17]: $\alpha h\nu = A(h\nu - E_g)^{1/2}$, where α is the absorption coefficient, $h\nu$ is the photon energy, E_g is the direct band gap energy, and A is a constant. As illustrated in Fig. 3b, the estimated band gap energy of ZnS nanospheres is about 3.62 eV, which is larger than that of common ZnS (bandgap of 3.54 eV). The observation of the blue shift in the band gap energy of ZnS nanospheres can be attributed to the reduced particle size showing quantum confinement effects[18], which is in agreement with the SEM results.

Since the photocatalytic activity is directly correlated to the surface area and pore structure of the photocatalyst, nitrogen adsorption-desorption measurements were carried out. Fig. 4 displays the nitrogen adsorption-desorption isotherms and the corresponding Barrett-Joyner-Halenda (BJH) pore-size distributions of ZnS nanospheres and common ZnS. A typical Type IV isotherm (Fig. 4a) indicates the presence of mesoporous structure in the ZnS nanospheres stemmed from the aggregation of nanoparticles. The inset of Fig. 4a shows the sharp and narrow pore size distribution with the pore diameter in the range of 3～4 nm, suggesting the uniform internal pore structures of ZnS nanospheres. The mesoporous structure was also observed in the common ZnS as presented in Fig. 4b. However, the pore size of common ZnS displays more irregular arrange from 2 to 20 nm (inset of Fig. 4b). Furthermore, the BET surface area of common ZnS is calculated to be 71.88 m^2/g, which is much lower than that of the as-prepared ZnS nanospheres (107.68 m^2/g).

3. 2 Photocatalytic properties

The photocatalytic activities of ZnS nanospheres and common ZnS were investigated by the degradation of methylene blue (MB) under UV-light irradiation, and the blank control experiment (pure MB solution without catalyst) was also evaluated under the same photocatalytic condition for comparison. Fig. 5a shows the time-dependent UV-vis absorption spectra for the degradation of MB under UV-light irradiation in the presence of ZnS nanospheres as a photocatalyst. It can be seen that the intensity of MB absorption peak around 664 nm decreases continually with an increase in the UV-light irradiation time and completely disappears after 25 min irradiation. As presented in Fig. 5b, the degradation ratio of MB has no significant increase for a long time in the presence of catalyst under dark conditions. Similar result of the blank control

experiment was also obtained. These results indicate that the light and catalyst are both necessary for effective photodegradation of MB dye, and the photoinduced self-decomposition of MB can be ignored in comparison with the photocatalytic degradation caused by catalyst in the solution. It is worth noting that the as-prepared ZnS nanospheres exhibit remarkable photocatalytic activity towards methylene blue degradation under UV-light irradiation. The degradation ratio of MB can reach up to 99.4% after irradiation for 25 min. In addition, ZnS nanospheres show much better activity than common ZnS for the photocatalytic degradation of MB. In comparison with common ZnS, the high photocatalytic efficiency of ZnS nanospheres can be ascribed to the larger specific surface area and hierarchical mesoporous structure, which can contribute to the diffusion and mass transportation of MB dye molecules and oxygen-containing radicals during the photocatalysis reaction[19].

4 CONCLUSION

In summary, well crystallized, mesoporous and zinc-blende ZnS nanospheres with uniform size were successfully obtained by a simple chemical process. It was found that the as-prepared ZnS nanospheres are assemblies of tiny nanoparticles and exhibit excellent photocatalytic activity with nearly 100% of MB degradation efficiency under UV-light irradiation for 25 min. The large specific surface area and hierarchical mesoporous structure of ZnS nanosphere are probably responsible for its excellent photocatalytic activity. The uniform and well-dispersed ZnS nanospheres can be used as a promising photocatalyst and hold great potential applications in wastewater treatment for the photodegradation of organic pollutants. This work provides insight into designing high-performance photocatalysts by constructing the complex architectures.

REFERENCES

(1) Yin, L.; Wang, D.; Huang, J.; Cao, L.; Ouyang, H.; Yong, X. Morphology-controllable synthesis and enhanced photocatalytic activity of ZnS nanoparticles. *J. Alloys Compd*. **2016**, 664, 476-480.

(2) Chen, F. J.; Cao, Y. L.; Jia, D. Z. Facile synthesis of ZnS nanoparticles and their excellent photocatalytic performance. *Ceram. Int.* **2015**, 41, 6645-6652.

(3) Soltani, N.; Saion, E.; Yunus, W. M. M.; Navasery, M.; Bahmanrokh, G.; Erfani, M.; Zare, M. R.; Gharibshahi, E. Photocatalytic degradation of methylene blue under visible light using PVP-capped ZnS and CdS nanoparticles. *Solar Energy*. **2013**, 97, 147-154.

(4) Yang, Y.; Huang, J. M.; Liu, S. Y.; Shen, J. C. Preparation, characterization and electroluminescence of ZnS nanocrystals in a polymer matrix. *J. Mater. Chem.* **1997**, 7, 131-133.

(5) Rajesh.; Sarkar, T.; Mulchandani, A. Photo-induced charge transport in ZnS nanocrystals decorated single walled carbon nanotube field-effect transistor. *Appl. Phys. Lett.* **2011**, 99.

(6) Guijarro, N.; Campina, J. M.; Shen, Q.; Toyoda, T.; Lana-Villarreal, T.; Gomez, R. Uncovering the role of the ZnS treatment in the performance of quantum dot sensitized solar cells. *Phys. Chem. Chem. Phys.* **2011**, 13, 12024-12032.

(7) Hu, P. F.; Gong, G. D.; Zhan, F. Y.; Zhang, Y.; Lic, R.; Caod, Y. L. The hydrothermal evolution of the phase and shape of ZnS nanostructures and their gas-sensing properties. *Dalton Trans.* **2016**, 45, 2409-2416.

(8) Dong, F. F.; Guo, Y. M.; Zhang, J.; Li, Y. H.; Yang, L.; Fang, Q. L.; Fang, H.; Jiang, K. Size-controllable hydrothermal synthesis of ZnS nanospheres and the application in photocatalytic degradation of organic dyes. *Mater. Lett*. **2013**, 97, 59-63.

(9) Moore, D. F.; Ding, Y.; Wang, Z. L. Crystal orientation-ordered ZnS nanowire bundles. *J. Am. Chem. Soc.* **2004**, 126, 14372-14373.

(10) Jiang, F. H.; Zhang, J. Synthesis and characterization of ZnS nanobelts based on substitution reaction. *Appl. Phys. A* **2011**, 105, 411-416.

(11) Chen, X. J.; Xu, H. F.; Xu, N. S.; Zhao, F. H.; Lin, W. J.; Lin, G.; Fu, Y. L.; Huang, Z. L.; Wang, H. Z.; Wu, M. M. Kinetically controlled synthesis of wurtzite ZnS nanorods through mild thermolysis of a covalent organic-inorganic network. *Inorg. Chem.* **2003**, 42, 3100-3106.

(12) Fang, X. S.; Ye, C. H.; Peng, X. S.; Wang, Y. H.; Wu, Y. C.; Zhang, L. D. Large-scale synthesis of ZnS nanosheets by the evaporation of ZnS nanopowders. *J. Cryst. Growth* **2004**, 263, 263-268.

(13) Bai, W. B.; Cai, L. F.; Wu, C. X.; Xiao, X. Q.; Fan, X. L.; Chen, K. Z.; Lin, J. H. Alcohothermal synthesis of flower-like ZnS nano-microstructures with high visible light photocatalytic activity. *Mater. Lett.* **2014**, 124, 177-180.

(14) Zhao, Q. R.; Xie, Y.; Zhang, Z. G.; Bai, X. Size-selective synthesis of zinc sulfide hierarchical structures and their photocatalytic activity. *Cryst. Growth Des.* **2007**, 7, 153-158.

(15) Yang, J.; Peng, J. J.; Zou, R. X.; Peng, F.; Wang, H. J.; Yu, H.; Lee, J. Y. Mesoporous zinc-blende ZnS nanoparticles: synthesis, characterization and superior photocatalytic properties. *Nanotechnology* **2008**, 19.

(16) Park, J. Y.; Park, S. J.; Lee, J. H.; Hwang, C. H.; Wang, K. J.; Jin, S.; Choi, D. Y.; Yoon, S. D.; Lee, I. H. Synthesis and characterization of cauliflower-like ZnS microspheres by simple self-assembly method. *Mater. Lett.* **2014**, 121, 97-100.

(17) Liu, S. H.; Qian, X. F.; Yin, J.; Ma, X. D.; Yuan, J. Y.; Zhu, Z. K. Preparation and characterization of polymer-capped CdS nanocrystals. *J. Phys. Chem. Solids* **2003**, 64, 455–458.

(18) Reddy, D. A.; Sambasivam, S.; Murali, G.; Poornaprakash, B.; Vijayalakshmi, R. P.; Aparna, Y.; Reddy, B. K.; Rao, J. L. Effect of Mn co-doping on the structural, optical and magnetic properties of ZnS:Cr nanoparticles. *J. Alloys Compd.* **2012**, 537, 208-215.

(19) Lei, A. H.; Qu, B. H.; Zhou, W. C.; Wang, Y. G.; Zhang, Q. L.; Zou, B. S. Facile synthesis and enhanced photocatalytic activity of hierarchical porous ZnO microspheres. *Mater. Lett.* **2012**, 66, 72-75.

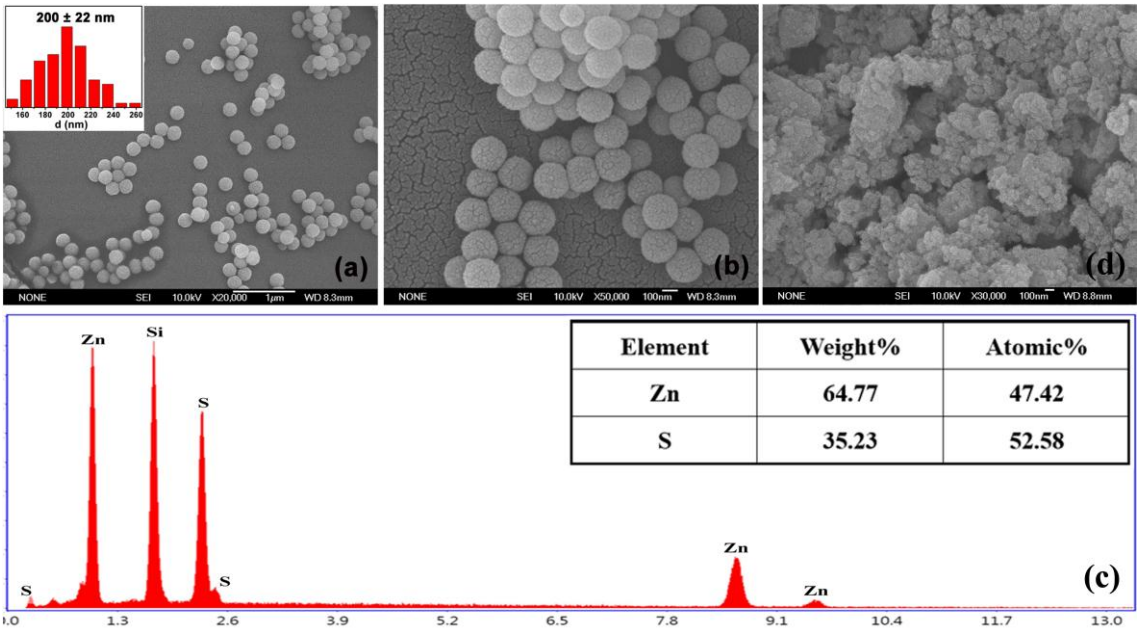

Fig. 1. (a) SEM image, (b) Enlarged SEM image,

and (c) EDS spectrum of ZnS nanospheres. (d) SEM image of common ZnS

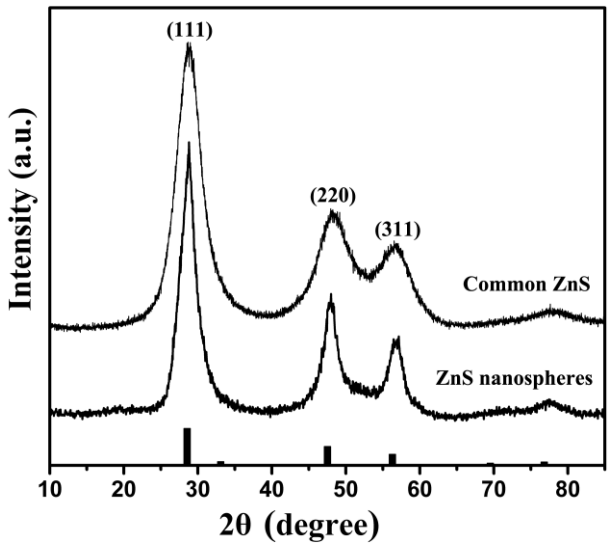

Fig. 2. XRD patterns of ZnS nanospheres and common ZnS.

Vertical bars at the bottom denote the standard data for a zinc-blende structure of ZnS (JCPDS, No. 05-0566)

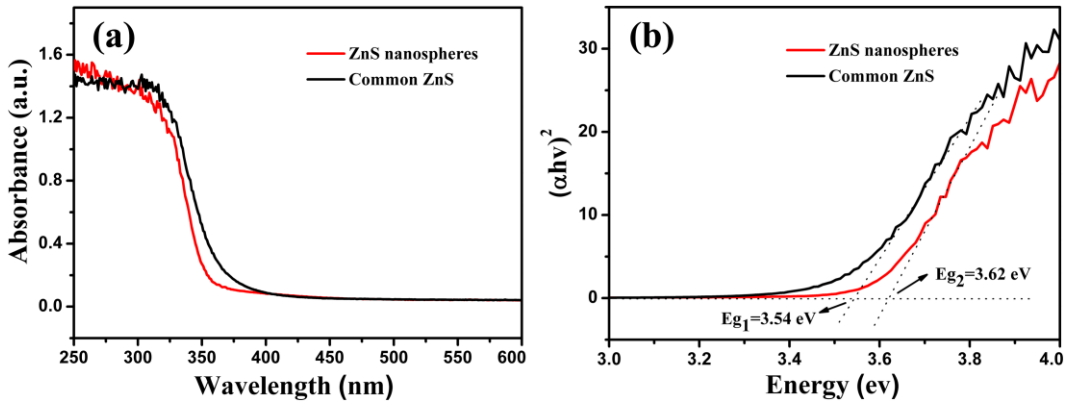

Fig. 3. (a) UV-vis absorption spectra of ZnS nanospheres and common ZnS, and (b) Plots of $(\alpha h\nu)^2$ *vs.* photon energy ($h\nu$) for ZnS nanospheres and common ZnS

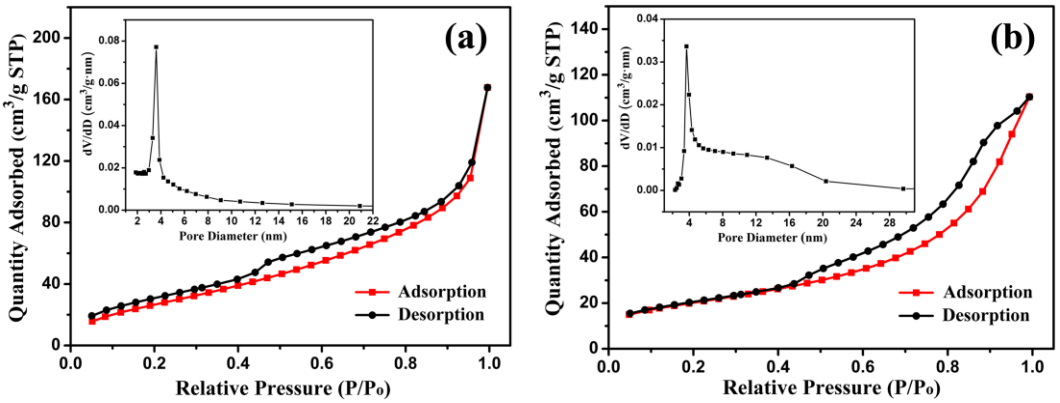

Fig. 4. Nitrogen absorption-desorption isotherm of (a) ZnS nanospheres and (b) Common ZnS. The insets correspond to the pore size distributions of the samples

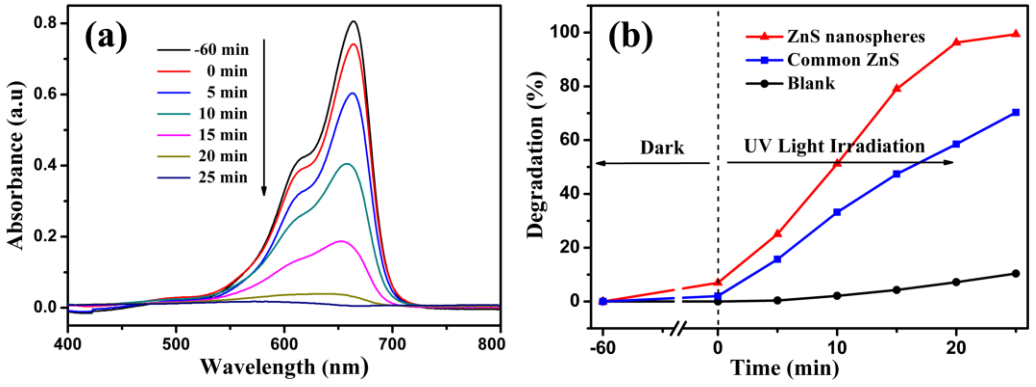

Fig. 5. (a) Time-dependent UV-vis absorption spectra for the degradation of MB over ZnS nanospheres under UV-light irradiation. (b) Degradation ratios of MB over ZnS nanospheres and common ZnS under UV-light irradiation

Facile Synthesis of Uniform Zinc-blende ZnS Nanospheres with Excellent Photocatalytic Activity toward Methylene Blue Degradation

PENG Si-Yan(彭思艳)　YANG Liu-Sai(杨流赛)　LV Ying-Ying(吕英英)

YU Le-Shu(余乐书)　HUANG Hai-Jin(黄海金)　WU Li-Dan(吴丽丹)

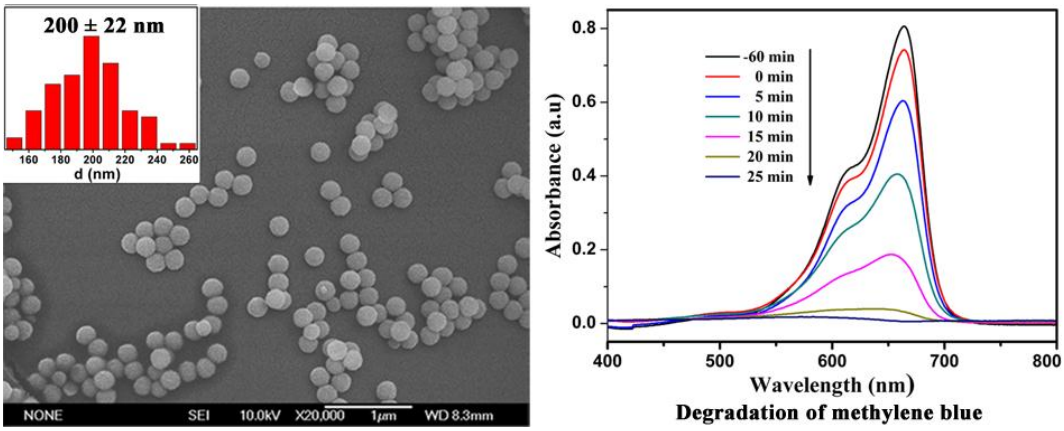

Uniform and well-dispersed ZnS nanospheres exhibit excellent photocatalytic activity toward methylene blue degradation. The large specific surface area and hierarchical mesoporous structure are responsible for their excellent photocatalytic activity.